# Application of Ultrasonic C-Scan Techniques for Tracing Defects in Laminated Composite Materials

**Hasiotis T., Badogiannis E. and Tsouvalis N.G.**
NATIONAL TECHNICAL UNIVERSITY OF ATHENS
School of Naval Architecture and Marine Engineering, Shipbuilding Technology Laboratory
Heroon Polytechniou 9, GR-157 73 Zografos, Athens, GREECE
badstrat@central.ntua.gr

***Abstract - In this paper practical ultrasonic C-scan techniques for NDT of laminated composite materials are developed and applied, aiming at tracing specific artificial defects. Two types of materials are examined, namely an advanced carbon/epoxy system with unidirectional fibers and a typical marine type glass/polyester system with woven roving reinforcement. Both materials were used in association with two manufacturing methods, namely the simple Hand Lay-Up method and the more advanced Vacuum Infusion one. Several artificial defects made of Upilex polyamide material were embedded into the test plates. These defects have varying shape and magnitude, as well as varying through thickness position, overlapping between each other in one case. A typical layer wrinkle was also manufactured at mid-thickness in each test plate. Test plates were C-scanned using an UltraPack II ultrasonic system in association with UltraWin software. The determination and characterization of defects was attempted by applying typical examination techniques, such as layer to layer examination, full width examination, etc. However, software tuning procedures and appropriate examination strategies were applied, in order to further develop and optimize the scanning procedure. These efforts resulted in effective C-scan images, allowing the determination of the position and, in some cases, of the size of the defects. Finally, precise determination of specimens' thickness was also achieved.***

**Keywords:** Composites, Ultrasonic, C-scan, Defects.

## 1 Introduction

In the last 30-40 years fibre composite materials have seen a growing popularity in a wide spectrum of industries. The pleasure boats industry is making extensive use of composites for some decades. Areas of higher-technology applications include aircraft and spacecraft structures. With a decreasing material price for the most commonly used fibre and resin types, composite materials have more recently been applied on a larger scale in ships and marine structures in general. It is the need for reducing the weight of the structure, in order to increase the strength-to-weight and stiffness-to-weight ratios, which rises the use of composite materials. Other advantageous properties include good thermal and acoustic insulation, low fatigue and corrosion and easy manufacturing of aero and hydrodynamically optimised shapes [1].

Defects are defined as any deviation from the nominal, ideal or specified geometric and/or physical make-up of a structure or component and, for the laminated composite materials, arise most frequently during the manufacturing procedure. Manufacturing defects can evolve to damage during the service life of a structure. Delamination is a defect type frequently met in composite materials, described as the separation of a layer or group of layers from their adjacent ones, due to failure of the internal bonding between the layers. Delamination can be either local or covering a wide area. It can occur either during the curing phase of the resin in the manufacturing stage or during the subsequent service life of the laminated part. Delaminations constitute a severe discontinuity, because they do not transfer interlaminar shear stresses and, under compressive loads, they can cause rapid and catastrophic buckling failure [1,2].

Ultrasonic inspection is a method used for quality control and materials quality inspection in all major industries. This includes electrical and electronic components manufacturing, production of metallic and composite materials and fabrication of structures such as airframes, piping and pressure vessels, ships, bridges, motor vehicles, machinery and jet engines. In-service ultrasonic inspection for preventive maintenance is also used for detecting any defects and impending failure in numerous structures, like railroad-rolling-stock axles, press columns, earthmoving equipment, mill rolls, mining equipment, nuclear systems and other machines.

The pulse-echo method, which is the most widely used ultrasonic method, involves the detection of echoes produced when an ultrasonic pulse is reflected from a discontinuity or an interface of a test piece. This method is very often used for flaws location and thickness measurements. C-scan display records echoes from the internal portions of test pieces as a function of the position of each reflecting interface within an area. Flaws are shown on a read-out, superimposed on a plan view of the test piece and both flaw size (flaw area) and position within the plan view can be recorded. Flaw depth normally is not recorded, although a relatively accurate estimate can be made by restricting the range of

depths (gates) within the test piece that is covered in a given scan [3].

In the literature there are many applications of the ultrasonic C-scan technique for the inspection of composite materials, mainly in carbon/epoxy systems, the use of which in advanced structures justifies the cost of such inspections. To name a few of these applications, the technique has been used to characterize artificial delaminations [4], to detect impact damage in carbon/epoxy composite plates [5], to characterize the distribution, size and shape of voids in composite materials [6] and to reveal some special features of the fiber/matrix interface [7].

The clustering procedure was applied in the present study in order to facilitate dimensioning of the detected defects. Clustering is an algorithm and thus a software supported process, in which a set of data is organized in groups that have strong similarities. The objective of clustering procedures is to find natural groupings of the data under study [2].

In this paper ultrasonic inspection of composite specimens is performed in order to locate several artificial defects, made of Upilex polyamide material. Two material types and two manufacturing methods were used, in order to investigate their effect on the effectiveness of the inspection method. In parallel, the two different materials would reveal any possible special features of the U/S software calibration that are needed for an effective inspection. The defects are simulating typical composite delaminations and they were embedded into the 14 layers test laminates. Their varying shape and size, as well as their varying location in the thickness direction of the laminate, overlapping between each other in one case, have as a result several delamination types, which in turn constitute different ultrasonic tracking cases. Appropriate tuning of the device software resulted in effective C-scan images, allowing the determination of the position and, in some cases, of the size of the defects, as well as the determination of the specimen thickness.

# 2 Experimental

## 2.1 Materials

Two types of materials were investigated, namely a typical marine glass/polyester composite (GFRP) and an advanced carbon/epoxy system (CFRP). In addition, two manufacturing methods were used, the simple and conventional in the marine industry Hand Lay-Up method (HLU) and the more advanced Vacuum Infusion method (VI). The combination of the aforementioned two materials and two manufacturing methods resulted in the preparation of totally four test laminates.

GFRP test laminates were manufactured using the typical polyester resin NORSODYNE G 703 from GRAY VALLEY, exhibiting a viscosity of 3200 mPa.s at 25°C and a specific weight of 1.17 g/cm$^3$, in association with a woven roving glass reinforcement having a weight of 500 g/m$^2$. CFRP test laminates were manufactured using the cold cured epoxy resin DER 358 from DOW, exhibiting a viscosity of 600-700 mPa.s at 25°C and a specific weight of 1.14 g/cm$^3$, in association with a 205 g/m$^2$ unidirectional carbon fibers reinforcement from HEXCEL. The same polyester resin and the same epoxy resin were used to manufacture the corresponding test laminates with both manufacturing methods. All four resulting laminates had 14 layers each. The artificial defects that were embedded in-between the layers of the test laminates were in the form of a very thin (12.7 μm) sheet, made of Upilex polyamide material.

## 2.2 Geometry of specimens

The four test laminates had dimensions 300 x 250 mm, as it is shown in Figure 1. Two specimens were cut from each test laminate, each one having dimensions 100 x 150 mm. The first specimen (on the left in Figure 1) is a reference specimen without any polyamide artificial defects and the second (on the right in Figure 1) included all the embedded polyamide artificial defects. In GFRP laminates, the woven roving fiber reinforcements were layered with their warp direction along y axis, whereas in CFRP laminates, the unidirectional fiber reinforcements were layered with their warp direction along x axis.

In total eight separate polyamide artificial defects were embedded in each one of the defected specimens. These defects, designated D1 to D8 (see Figure 1), had the specific dimensions and were placed at the specific x-y positions shown in Figure 1. The distances between these defects were chosen so that their presence does not influence the detection of their neighbor ones. More specifically, the detailed characteristics of all these defects are as follows:

- D1: circular shape, radius = 5 mm, embedded between layers No. 4 and 5 (layers numbering starts from the mould side of the test laminate).
- D2: square shape, side = 10 mm, embedded between layers No. 4 and 5.
- D3: circular shape, radius = 10 mm, embedded between layers No. 4 and 5.
- D4: square shape, side = 20 mm, embedded between layers No. 4 and 5.
- D5: circular shape, radius = 10 mm, embedded between layers No. 3 and 4 (solid line in Figure 1).
- D6: circular shape, radius = 5 mm, embedded between layers No. 7 and 8 (dashed line in Figure 1).
- D7: circular shape, radius = 5 mm, embedded between layers No. 3 and 4 (solid line in Figure 1).
- D8: circular shape, radius = 10 mm, embedded between layers No. 7 and 8 (dashed line in Figure 1).

Defects D1 to D4 were placed at the same position through thickness, at a distance of approximately 30% of the total thickness from the mould surface of the laminate. Their objective was to investigate the capability of the method and the software settings required to detect the shape of the defects (square versus circular) and this be done for two different magnitudes (smaller and larger). Moreover, their non-symmetric placement through thickness would enable the

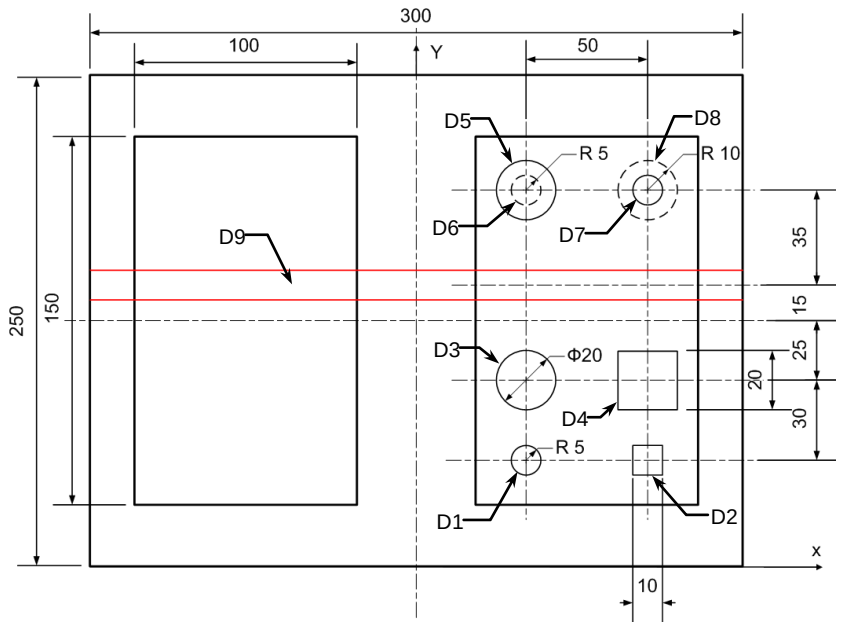


Figure 1 : Layout of specimens with artificial defects

investigation of the effectiveness of the method when trying to detect these defects from both sides of the laminate. Unfortunately, the relatively rough free surface of all test laminates (the surface not in contact with the mould) did not enable the performance of ultrasonic inspections from this side, due to the many signal reflections. Thus, all ultrasonic measurements and inspections reported in the following were performed from the smooth side of the specimens that was in contact with the mould.

The objective of defects D5 to D8 was somewhat different. Defects D5 and D6 are placed through thickness in reverse order with respect to defects D7 and D8. The aim here was to investigate the capability of the method to detect and distinguish two overlapping defects of different size. These latter four defects were on purpose not placed at symmetric through thickness positions, in order to try to detect them from both sides of the laminate.

In addition to the above eight polyamide defects, a ninth one was manufactured (D9), consisting of a wrinkle of the sixth layer from the mould surface, along the full length of the test laminate (see red lines zone in Figure 1). The width of this wrinkle was varying from 10 to 15 mm. In the GFRP test laminates, this type of defect was manufactured by cutting the sixth layer in two pieces and overlapping them, since it was very difficult to create such a small wrinkle with a woven roving glass reinforcement. The objective of defect D9 was to investigate the capability of the method to detect and dimensionalize such types of defects, which are common in typical marine composite structures.

The actual thicknesses of all eight specimens are listed in Table 1, measured by conventional methods (caliper and micrometer). Values are given for both the nominal average uniform thickness of each specimen, as well as for the increased thickness at the area of the wrinkle. The listed thicknesses are average values from five measurements in the case of the uniform thickness and from two measurements in the case of the thickness at the wrinkle.

Table 1 : Thickness of specimens

| Specimen | Average uniform thickness (mm) | Thickness at wrinkle (mm) |
|---|---|---|
| CFRP-HLU | 7.49 | 7.84 |
| CFRP-VI | 3.00 | 3.28 |
| GFRP-HLU | 8.28 | 8.86 |
| GFRP-VI | 5.45 | 5.84 |

## 2.3 Device and equipment set-up

The ultrasonic inspection of the specimens was made by applying the Pulse – Echo method. A ¼´´ diameter single crystal pulse-receiver flat transducer of 5 MHz from PANAMETRICS was used and the inspection was made with the specimens immersed in distilled water. The ultrasonic device used is ULTRAPAC II system (automated immersion system), in association with ULTRAWIN software for data acquisition, control and imaging [8].

Special techniques and tuning procedures were applied for the ultrasonic inspection of the various specimens. As it is commonly done, the distance between the transducer and the material (water path) was set at the end of the near field value of the transducer used (which is 33.2 mm), in order to avoid the fluctuation of the acoustic pressure which takes place into the near field zone [2]. A glass plate, on which the specimens were placed, was used as a reflective plane, in order to distinguish the backwall echo from any other one [9].

The four reference specimens without defects were used for the determination of the sound velocity inside all types of materials. For this to be done, an initial constant sound velocity was considered (i.e. that of steel) and an

U/S dummy thickness measurement was performed at each specimen. In the sequence, the actual sound velocity was calculated by comparing this dummy thickness to the actual thickness of each specimen (see Table 1) [10]. The sound velocity calculated in this way was equal to 2.90 mm/ms in the case of the CFRP specimens and 2.79 mm/ms in the case of the GFRP ones.

A linear Distance Amplitude Correction (DAC) curve was used in order to increase the ultrasonic signal amplitude, thus facing the signal losses owing to factors like scattering, absorption, etc.[11]. The gates were synchronized with the first echo from the specimen and the detection threshold was adjusted to a value above 20% of the Full Screen Height (FSH), thus avoiding the produced noise echoes. Depending on the nature of each defect to be detected, as well as on the area of interest to be inspected (i.e. layer by layer or backwall inspection), a detailed study was done aiming at selecting the most effective detection strategy. Four common strategies were studied, namely max-peak, max-thres, first-peak and first-thres.

# 3 Results and discussion

Due to space limitations, in the present study results are presented only for the CFRP and the GFRP specimens manufactured with the vacuum infusion method.

## 3.1 CFRP specimens

Figure 2 presents the Time Of Flight (TOF) C-scan of the CFRP specimen with defects. The gate was placed at backwall echo and the first-peak strategy was used in order to measure the thickness of the specimen. The thickness variation is presented in Figure 2 with different colors (see legend on the left). The gate width was properly adjusted in order to monitor the maximum thickness value of the wrinkle (see Table 1). Figure 2 shows that the majority of the specimen thickness is around the nominal value of 3 mm (green color), however there are areas where thickness is larger, like those around and on the artificial defects and at the wrinkle (blue and red color). The horizontal orthogonal white color zone indicates that the wrinkle area has thickness greater than 3.28 mm. The two circular white zones owe to the existence of the two different sized, overlapping defects (D5, D6 and D7, D8), which cause the absorption of a big amount of the acoustic energy and, therefore, no data points are reported there. In the B and B´ scans shown in the horizontal and the vertical axis of the image, respectively, the thickness variation along the shown cross hair lines is presented. The aforementioned no data areas are monitored also in these scans.

In Figure 3 the amplitude C-scan of the CFRP specimen with defects is shown. The gate was properly adjusted in order to inspect the area from the top of the 3rd layer to the bottom of the 5th layer. The max-peak strategy has been applied in order to monitor all defects which have initially been placed between the 3rd and the

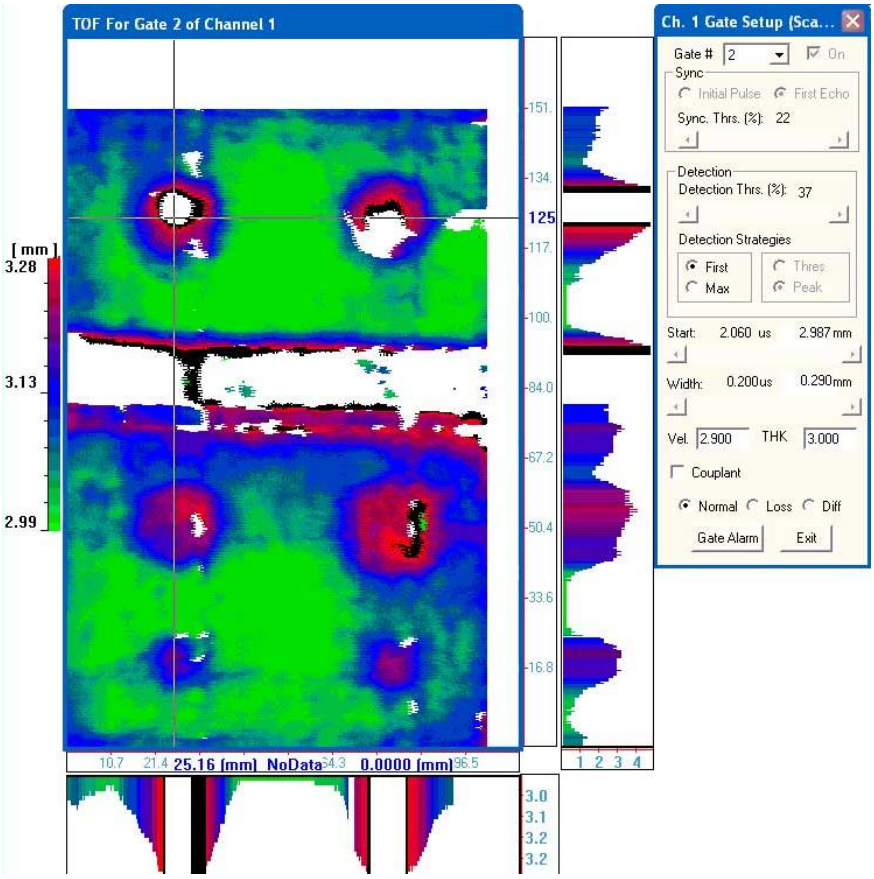

Figure 2 : TOF C-scan of CFRP-VI specimen focused at backwall

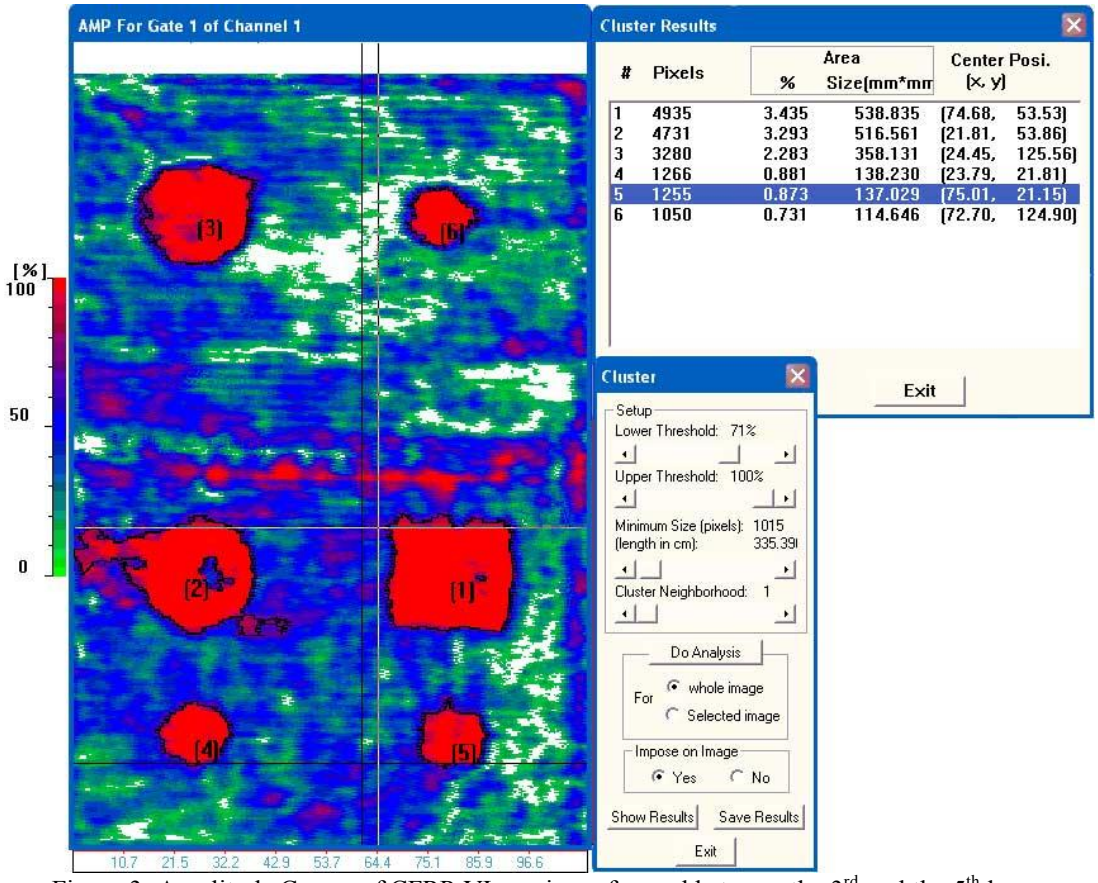


Figure 3: Amplitude C-scan of CFRP-VI specimen focused between the 3rd and the 5th layer.

4th layer, that is all defects except D6 and D8. These six defects are clearly shown in Figure 3. The same figure shows also clearly the direction of the fibers, which is parallel to the short side of the specimen.

In the sequence, the cluster analysis utility of the software was used, in order to determine the dimensions and the position of each defect and compare these values to the initially defined ones, before the construction (see Figure 1). The clustering procedure was applied to isolate group of data with amplitude greater than 70% of FSH, which correspond to defects. The aim of this analysis is to conclude on whether the applied procedure is able to accurately estimate the defects dimensions, as well as to define if the manufacturing procedures influenced the final position of the defects.

The last two columns of the "Cluster Results" window in Figure 3 present the monitored data for the co-ordinates of the center of each defect (defects numbering is shown in the figure), where x- and y- axes origin is at the lower left corner of the picture. The comparison of these data to the corresponding initial values shown in Figure 1 leads to the conclusion that the defects remain almost in the same position as they have been placed during the construction phase. Moreover, it is shown that the applied method scanned accurately the shape of each defect.

The "Cluster Results" window in Figure 3 presents also the ultrasonically monitored area of each defect (fourth column). By comparing these values to the original defect areas that can be calculated from Figure 1, we see that the ultrasonic method significantly overestimates the area of all defects, from 14 up to 73%. These differences may probably owe to the fact that all layers above the artificial defects exhibit a small bending over the defects. As a result, echoes from the areas adjacent to the defects are amplified up to 70% of FSH and they are recognized as defect areas.

In Figure 4, a 3-D amplitude C-scan of the CFRP specimen is given, focused from the 3rd down to the 5th layer. The six defects of the specimen D1, D2, D3, D4, D5 and D7 are clearly shown in this figure. They are colored in red, since these areas are highly reflective to the acoustic energy.

## 3.2 GFRP specimens

For the GFRP specimen, max-peak strategy was applied and TOF was measured in order to determine the through thickness position of the peaks with maximum amplitude. In general, increased amplitude of peaks implies the existence of defects. On the other hand, increased amplitude areas are also monitored because of the high reflectivity of glass fibers.

Figure 5 shows the TOF C-scan of the GFRP specimen, focused at the 3rd layer in order to detect defects D5 and D7. The echoes coming from the glass fibers result in a more or less uniform color motive of the inspected surface. In this respect, Figure 5 clearly shows the general pattern of the glass yarns, constituting the woven roving reinforcement. The orientation of the fibers is clearly shown. The echoes coming from the defects have the same TOF and, therefore, are much more

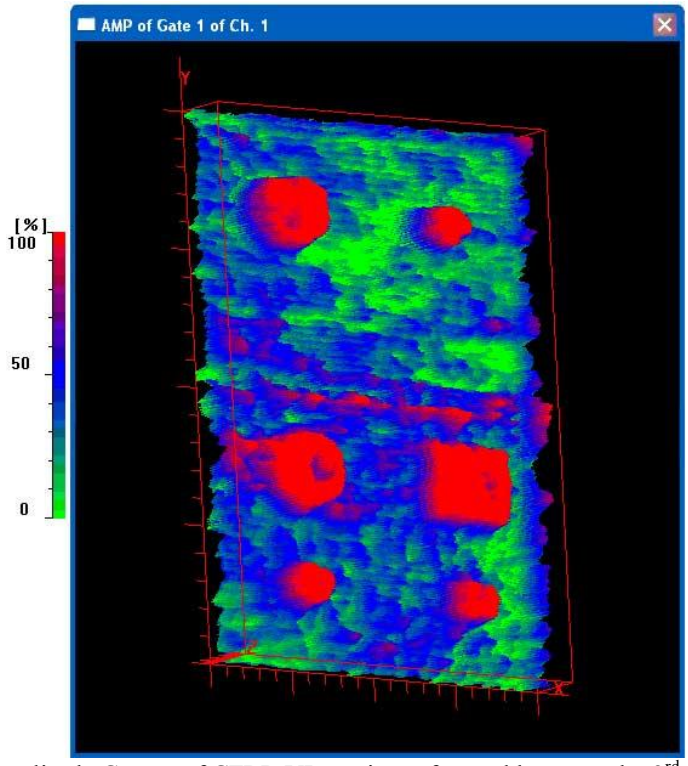


Figure 4: 3-D amplitude C-scan of CFRP-VI specimen focused between the 3rd and the 5th layer

concentrated and correspond to a single color (red areas in the figure). In order to better define these areas, we also take into account that their size must be considerably larger than the size of the repeated square crossings of the fibers in the warp and fill directions, whose dimension is approximately 4 mm.

However in the B and B′ images in the horizontal and vertical axis of the image, respectively, it is shown that these red areas are not clearly defined, but they are mixed together with the echoes coming from the glass fibers. Therefore, these areas do not have a specific shape and well defined borders, as it is evident from Figure 5.

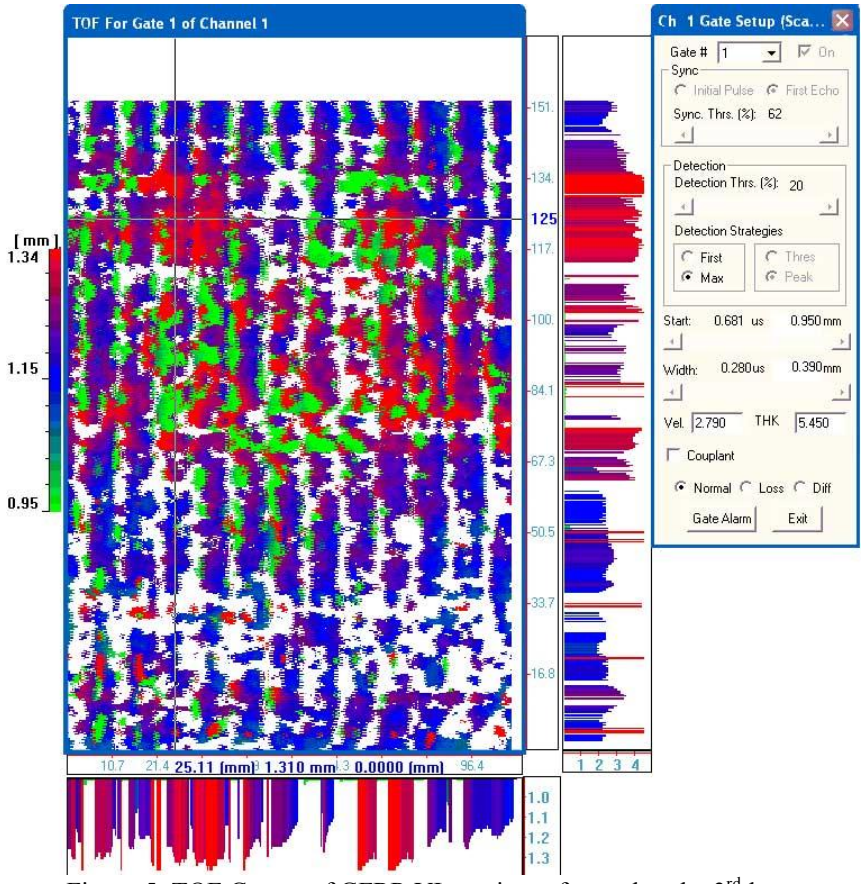


Figure 5. TOF C-scan of GFRP-VI specimen focused at the 3rd layer

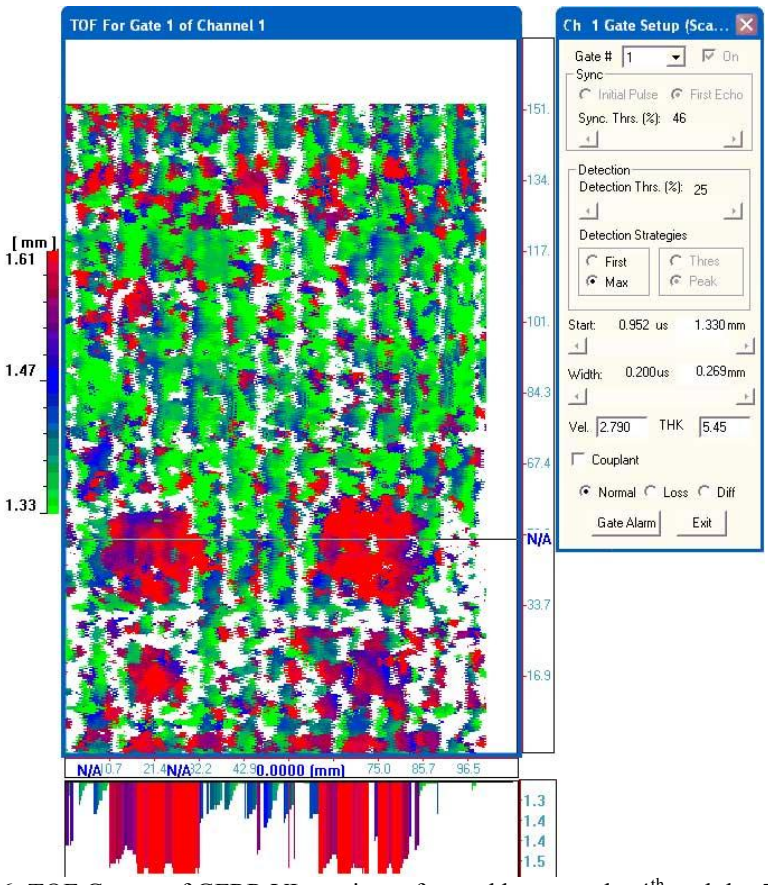


Figure 6. TOF C-scan of GFRP-VI specimen focused between the 4th and the 5th layer

Figure 6 shows the TOF C-scan of the GFRP specimen, focused at the area between the 4th and the 5th layer, in order to detect defects D1 to D4. The red colored areas, which correspond to the two aforementioned defects, are reported to a depth of approximately 1.6 mm, which is very close to the actual through thickness position of these defects. Although the existence of the defects is indicated in Figure 6, their geometry is once more not clearly defined, as was also the case in Figure 5.

In Figure 7, a 3-D TOF C-scan of the GFRP specimen is given, focused from the 4th down to the 5th layer. Contrary to the CFRP specimen case, the four defects D1 to D4 are not clearly defined in this figure. Echoes with high amplitude at the same TOF are monitored, but the shape of the resulting area is not geometrically specific.

## 4 Conclusions

The present study investigated the efficiency of the ultrasonic inspection method for detecting defects in laminated composite fibrous materials. The parameters of the study involved two different materials and two different manufacturing methods. The artificial defects were of various shape and size and were placed at various through thickness positions. The main conclusions that can be drawn out from this study are the following:

– The equipment used and the procedures applied proved much more efficient in the case of the CFRP specimens than when inspecting the GFRP ones. This happened due to the intense echoes that were reflected by the glass fibers, which were frequently overlapping the echoes coming from the actual defects. This phenomenon did not happen in the case of the carbon fibers.

– The method proved capable of accurately defining the position of the artificial embedded defects in the CFRP specimens. In the case of the GFRP specimens, position detection of these defects was less accurate, however satisfactory.

– The shape of the embedded defects was also accurately monitored in the case of the CFRP specimens. On the contrary, the shape of the defects in the GFRP specimens was not very well defined.

– Regarding the size of the defects, the method significantly overestimated their values in the case of the CFRP specimens, whereas it was not possible to estimate any size at all in the case of the GFRP ones.

– The wrinkle defect was accurately detected in the case of the CFRP specimens, whereas it was not detected at all in the case of the GFRP ones.

– The orientation of the fibers was clearly detected in both types of specimens.

– The ultrasonic inspection of the GFRP specimens would probably resulted in a much better representation of the actual situation if another sensor was used, having lower frequency (i.e. 3.5 MHz) and being focused. In this way, the scattering of echoes coming from the glass fibers would be considerably decreased.

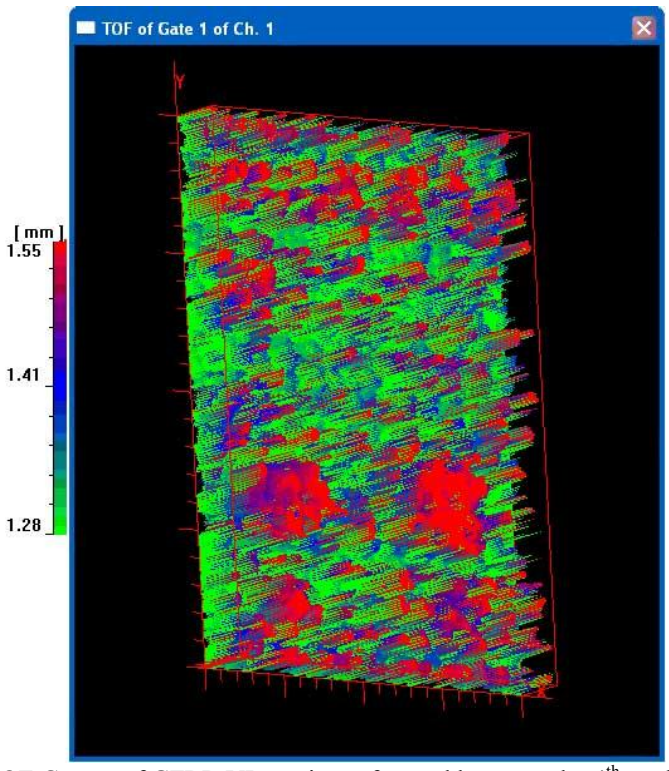


Fig 7. 3-D TOF C-scan of GFRP-VI specimen focused between the 4th and the 5th layer

## Acknowledgments

The authors gratefully acknowledge Messrs A. Markoulis and H. Xanthis, technical personnel of Shipbuilding Technology Laboratory, for their valuable contribution in the construction of the test laminates.

## References

[1] B. Hayman, C. Berggreen, A. Shenoi, N. Tsouvalis and P. Wright, *Production Processes, Production Defects and Production Process Modelling for FRP Single Skin and Sandwich Structures*, MARSTRUCT Network of Excellence Report No. MAR-W4-3-DNV-04(5), Jan 2007.

[2] *Non-destructive Testing Handbook*, 2nd Edition: Volume 7, Ultrasonic Testing, ASNT, 1991.

[3] *Non-destructive Evaluation and Quality Control*, ASM Handbook, Volume 17, 9th Edition, 1992.

[4] P.A. Lloyd, *Ultrasonic System for Imaging Delaminations in Composite Materials*, Ultrasonics, 27: 8-18, Jan 1989.

[5] K. Imielinska, M. Castaings, R. Wojtyra, J. Haras, Le Clezio and B. Hosten, *Air-coupled Ultrasonic C-scan Technique in Impact Response Testing of Carbon Fibre and Hybrid: Glass, Carbon and Kevlar/Epoxy Composites*, Journal of Materials Processing Technology, 157-158: 513-522, 2004.

[6] L. Liu, B.M. Zhang, D.F. Wang and Z.J. Wu, *Effects of Cure Cycles on Void Content and Mechanical Properties of Composite Laminates*, Composite Structures, 73: 303-309, 2006.

[7] J. Chang, C. Zheng and Q.-Q. Ni, *The Ultrasonic Wave Propagation in Composite Material and its Characteristic Evaluation*, Composite Structures, 75: 451-456, 2006.

[8] ULTRAWIN Software, User's Manual, Rev. 2.58, Oct 2002.

[9] D.J. Roth, *Using a Single Transducer Ultrasonic Imaging Method to Eliminate the Effect of Thickness Variation in the Image of Ceramic and Composite Plates*, Journal of Nondestructive Evaluation, 16(2): 101-119, 1997.

[10] I. Prassianakis, *NDT of materials. Ultrasonic Method*, NTUA, Athens, 2003.

[11] U. Pfeiffer and W. Hillger, *Spectral Distance Amplitude Control For Ultrasonic Inspection of Composite Components*, ECNDT 2006 - Mo.2.6.4.